Mapping the vulnerability to urban heat island combining satellite and ecosystem service data: a case study in Udine (Italy)

Davide Longato
Department of Architecture and Arts,
IUAV University of Venice
dlongato@iuav.it

Denis Maragno
Department of Architecture and Arts,
IUAV University of Venice
dmaragno@iuav.it

Received: October 2023
Accepted: March 2024

DOI: 10.13128/contest-14816

keywords
land surface temperature
urban green spaces
ecosystem service assessment
ecosystem service flows
remote sensing

Urban environments tend to experience higher temperatures than their rural surroundings, a phenomenon called urban heat island (UHI). Land Surface Temperature (LST) measurements are widely used to monitor surface UHI. Despite this, they are considered unsuitable to support effective UHI mitigation strategies since they cannot capture air mixing mechanisms contributing to determining the variability of urban air temperatures, which is the main parameter depicting urban thermal discomfort associated with UHI. Options to spatially assess air UHI exist but are based on

Introduction

Urban environments, especially the denser ones, are likely to experience higher temperatures than their rural surroundings, a phenomenon known as urban heat island (UHI) (Oke et al., 2017). Artificial infrastructure, buildings, and man-made structures having a high proportion of impervious paved surfaces (e.g., asphalt, concrete), which are mostly concentrated in urban areas, contribute to temperature increase by absorbing and re-emitting the Sun's heat more than natural and semi-natural areas landcover such as forests, water bodies, cropland, and urban green spaces (e.g., various authors in Yu et al., 2020). Furthermore, human activities (e.g., heating buildings, driving cars, heat released during industrial processes) also contribute to warming the surroundings, while narrow streets with a low sky view factor can trap heat by reducing air flow (Kim et al., 2022). All these factors contribute to the formation of UHI, which is most pro-

fine-scale local data observations or complex climate models. This study presents a simple and quick method to assess the vulnerability to UHI of urban areas that combines measurements of LST and an assessment of the cooling effects provided by ecosystems. The method is applied in the city of Udine (Italy). Results show the urban areas that are potentially more vulnerable to UHI and reveal the potentialities of the method in improving LST-based assessments to support UHI mitigation strategies. The method is then discussed in light of its advantages, limitations, and future improvements.

nounced at night when temperatures in urban areas can be significantly higher than in rural areas (e.g., Steigerwald et al., 2022). This is because during the night artificial structures such as buildings and roads slowly release back to the atmosphere the heat accumulated during the day; this process limits the natural decrease of temperatures during night hours in urban areas (Azevedo et al., 2016; Parker, 2010).

The UHI phenomenon is an important issue in cities since it exacerbates the negative impacts of high temperatures on human health, including cardiovascular and respiratory disorders, as well as heat stroke (Reiners et al., 2023). Living in a city during a heatwave is therefore particularly dangerous as people have to deal with the aggravating heat-related health consequences of this phenomenon. Hence, it becomes crucial to lower heat stress in urban environments by mitigating its effects.

Urban planners and local governments are called to design strategies and implement solutions to reduce this heat stress in cities (Aflaki et al., 2017). But to provide more effective outcomes and target the urban areas that are most in need of these solutions, they have to be informed about what areas should be prioritized because of more vulnerable to UHI effects.

The only rather simple, quick, and low-cost method to assess UHI effects at large spatial and temporal scales is through remotely-sensed spatially-explicit measurements of Land Surface Temperature (LST), which capture the land surface's contribution in determining the UHI phenomenon (i.e., the so-called surface UHI) and its spatially varying intensity (Reiners et al., 2023). Especially during heatwaves, and the summer period in general, the temperature of the land surface tends to be hotter than the temperature of the air, with building and pavement areas showing the highest surface temperatures, while water and green patches the

lowest (e.g., Tang et al., 2023; Wei and Wang, 2022). LST is often used as a relevant proxy to assess air UHI (Bird et al., 2022), also known as 'canopy UHI' or 'near-surface UHI' (e.g., Xiang et al., 2023; Azevedo et al., 2016). The urban canopy represents "the thin layer of the atmosphere between ground level and rooftop height and is strongly influenced by urban geometry and microscale energy exchange" (Azevedo et al., 2016). Measurements of air UHI are thus the primary information to support effective planning of solutions to mitigate UHI, since it is the most direct indicator of residents' perception and a crucial factor in evaluating urban thermal discomfort associated with UHI (Xiang et al., 2023) and, consequently, to health risks (Venter et al., 2021a).

However, despite the plenty of studies that focus on spatially-explicit assessments of surface UHI (e.g., Park and Cho, 2016), measurements of LST are often considered unsuitable to properly reflect the air UHI of a city and its spatially varying intensity (e.g., Shiflett et al., 2017). This is because LST data is not able to fully capture the thermal dynamics and air mixing mechanisms occurring in the air layers above the surface, which are driven by the complex thermal interactions between urban and vegetated land covers (Sun et al., 2020). Establishing a relationship between LST and air temperature, and consequently between surface UHI and air UHI, is therefore not so straightforward, given that LST measurements often neglect the micro-advection processes in the near-surface air layer that promote the mixing of the different thermal properties (i.e., warming and cooling air fluxes) generated across a wider area surrounding a specific location (various authors in Shiflett et al., 2017). Several authors (e.g., Xiang et al., 2023; Venter et al., 2021a) warn that using surface UHI as a proxy to evaluate air UHI with the ultimate objective of producing urban heat risk assessments and inform effective UHI mitigation strategies could be misleading given their non-linear relationship that leads to frequent overestimations of UHI effects by LST (e.g., Pena Acosta et al., 2023; Venter et al., 2021a).

On the other side, measurements of air temperature that can be directly used to assess UHI effects in cities are rather unlikely due to the limited distribution of urban weather stations, among others (Xiang et al., 2023). Other methods for measuring air temperature exist, but they are based on (occasional) field measurement campaigns requiring specific instruments, e.g., through mobile measurements (Schwarz et al., 2012), thus they are difficult to replicate in space and time.

To overcome the abovementioned issues related to LST and air temperature measurements for characterizing UHI risk in cities, during the last years several climate modeling tools (e.g., WRF model) integrating air temperature measurements and remotely-sensed LST data have been developed to estimate temperature variations in urban areas with high spatial resolution,

thus being able to capture UHI effects (Azevedo et al., 2016). However, the successful implementation of climate models depends on the availability of local observation data and time for initialization and verification meaning, as well as rather complex technical skills for setting and using the modeling tools; all aspects that often do not align with the decision-making context where urban planning decisions are formulated.

As anticipated, green areas made of natural and seminatural ecosystems and, more in general, vegetation, play a key role in mitigating UHI effects in cities by providing cooler air flows that can cool down temperatures in warmer urban environments. Depending on their typology and structure, green areas can provide more or less intense cooling effects that contribute to reducing temperatures locally. This benefit can also be denominated as 'local climate regulation' or 'microclimate regulation' service, among others, and is one among the regulating ecosystem services (ES) that most natural and seminatural ecosystems, with different intensities, can supply (e.g., Goldenberg et al., 2021; Zardo et al., 2017). These cooling effects are mainly delivered thanks to the shading and evapotranspiration processes of vegetation that mask downward solar radiation and absorb latent heat (Park et al., 2021). From the areas of ES provision, the cooling effects can flow (through natural air movement) towards and benefit the nearby areas (Goldenberg et al., 2021), through the so-called (distance) decay effect or function (e.g., Geneletti et al., 2016; Zardo et al., 2017), which is a critical factor to consider when supporting strategies to mitigate UHI effects in cities (e.g., green space planning/design) (e.g., Longato et al., 2023).

This study proposes a method that can be rather easily and quickly deployed at no cost to spatially assess the vulnerability of urban areas in relation to their propensity to suffer from more or less intense UHI effects by combining LST measurements with a simple spatial simulation of the ecosystem's cooling benefits. The study aims to provide a step-by-step procedure that can be used in the absence of more sophisticated methods (e.g., air temperature measurements or climate modeling tools). It attempts to enhance the quality of satellite-based proxy information for assessing UHI vulnerability in cities by capturing some of the possible near-surface air mixing processes that are not fully accounted for in the assessment that uses the LST data only. The method is applied in the city of Udine (Italy) but is potentially replicable worldwide.

Case study

The case study is represented by the city of Udine (Italy), a medium-sized city of 97,887 inhabitants (ISTAT, 2023) located in the Friuli Venezia Giulia region, at the north-eastern borders of the Po Valley area.

According to the land use and cover map (Figure 1), Udine is characterized by a rather compact ur-

Overview of the main land use and cover classes in the municipal area of Udine
Credits: elaboration of the authors
Fig. 1

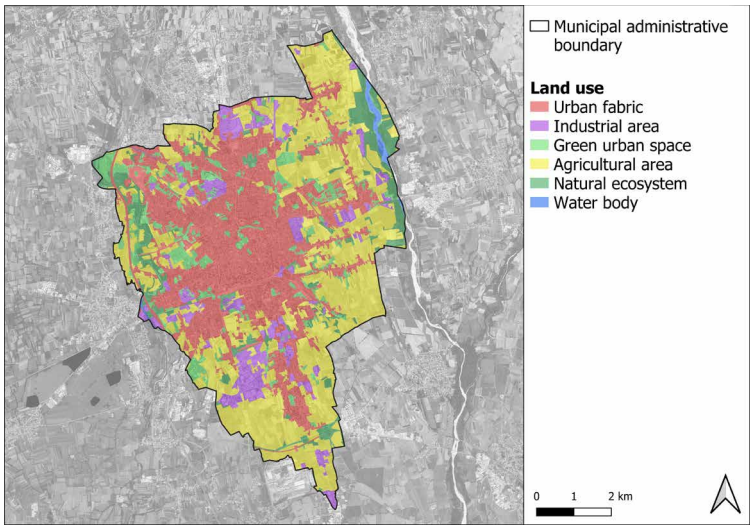

ban structure with dense urban fabric and scattered urban green areas, which are not evenly distributed but mainly located north of the city center. Industrial areas are especially located in the southern and northern peri-urban borders. Few natural areas are disseminated within the rural surroundings, often characterized by high fragmentation and small size. Only the areas lying along the two rivers flowing east and west of the city are characterized by a more significant presence of natural ecosystems.

Concerning the climatic profile of the city we can observe the following characteristics according to the regional climate report (ARPA FVG, 2023). The city is located in one of the regional areas with the highest annual temperature variation and the hot days (i.e., days in which the temperature reaches 30°) are usually between 40 and 50 in a year. Maximum temperature values are typically registered during July and August. There are two precipitation peaks in a year: one in late-spring/early-summer (May and June) and one in autumn (especially November). However, all over the year, the precipitations are not scarce with an average of 1,500 mm and a minimum registered in February (60-90 mm). However, during the summer season, precipitations are mainly originated from rainstorm events with heavy rain in a relatively short time, which alternate with dry periods that can last up to two weeks without rain.

Data and methods

The spatially explicit assessment of the vulnerability of the urban area of Udine in relation to

its propensity to suffer from UHI effects is carried out by combining two major factors contributing to the UHI spatially varying intensity: i) the first is related to the urban land surface's contribution in determining the UHI phenomenon; ii) the second is related to the possibility to benefit from cooling effects flowing from nearby ecosystems that can locally cool down temperatures.
According to the IPCC risk assessment framework, the vulnerability of a system can be described as its "propensity or predisposition to be adversely affected. Vulnerability encompasses a variety of concepts and elements including sensitivity or susceptibility to harm and lack of capacity to cope and adapt" (IPCC, 2014). Among the two factors considered in the proposed vulnerability assessment, the first can be considered as a factor depicting the sensitivity (i.e., "the degree to which a system is affected [...] by climate-related stimuli" (IPCC, 2007)) of the urban area to UHI. The second can be considered as a factor depicting the coping capacity (i.e., "the ability [...] to manage adverse conditions" (UN, 2016)), namely the capacity to cope with the adverse effects of UHI thanks to the ecosystem's ability to mitigate high temperatures.

To assess the factor related to the urban land surface's contribution in determining the UHI phenomenon, the remotely-sensed data of Land Surface Temperature (LST) was used. The LST is derived from satellite images acquired by the platform Landsat 8, which – to date – provides the most accurate (in terms of spatial resolution, corresponding to 30x30 meters) thermal data that is freely accessible among the ongoing satellite missions.
The LST data used in the assessment was elaborated using the Google Earth Engine platform, which allows the elaboration of a large amount of (satellite) data in a relatively small amount of time taking advantage of the elaboration power of Google servers. This way, it was possible to use the whole time series of available Landsat 8 images covering the case study area (from 2013 – launch of the Landsat 8 mission – to 2022) to calculate the average LST during the summer season (i.e., months of June, July, and August).
The average LST summer values were subsequently re-classified into five classes depicting the different sensitivity to UHI. To do so, five different ranges of LST values (subsequently called 'LST classes') were obtained by categorizing the LST values into five quantiles in a GIS environment (i.e., using the "Natural breaks (Jenks)" statistical method that clusters data into groups that minimize the within-group variance and maximize the between-group variance). Scores from 1 to 5 – corresponding to the increasing sensitivity condition – were assigned to the LST classes according to the increasing LST values (Table 1).

To assess the factor related to the possibility of benefiting from cooling effects flowing from

LST class (quantiles)	Sensitivity	Score
> 41.82°	Highest	5 (worst condition)
39.55° - 41.82°		4
38.06° - 39.55°		3
36.57° - 38.06°		2
< 36.57°	Lowest	1 (best condition)

LST classes and associated sensitivity conditions with corresponding scores

Tab. 1

Cooling benefits (qualitative score)	Coping capacity	Score
Not benefitting from any cooling effect (0)	Null	5 (worst condition)
Benefitting from cooling effects with low (1) to moderate (2) cooling intensity potential		4
Benefitting from cooling effects with medium (3) cooling intensity potential		3
Benefitting from cooling effects with high (4) cooling intensity potential		2
Benefitting from cooling effects with very high (5) cooling intensity potential	Highest	1 (best condition)

Cooling benefits according to cooling intensity potential and associated coping capacity conditions with corresponding scores

Tab. 2

nearby ecosystems, thus the capacity to cope with the adverse effects of UHI, the following procedure was adopted.

First, the potential to provide the local climate regulation service by ecosystems was assessed by using the matrix developed by Burkhard and colleagues (2014), in which for each Corine Land Cover class a qualitative score (from 0, null, to 5, highest potential; elaborated starting from expert judgments) depicting ES potential (supply) is assigned for provisioning, regulating, and cultural ES. Concerning the local climate regulation service, the highest ES potential is provided by woodland areas, followed by shrubland, agricultural areas with significant natural elements, arable land and natural grassland, pastures, and permanent crops (for more details see the ES potential matrix in Burkhard et al. (2014)). To this aim, the regional Habitat Map (updated in 2021) was used, being preferred to the Corine Land Cover map since more updated and with higher spatial resolution. To apply the matrix and assign the scores in the case study area, the habitat categories of the Habitat Map were converted into the corresponding Corine Land Cover classes using the conversion matrix elaborated by the European Environment Agency.

Second, the urban areas potentially benefitting from this ES – which spatially radiates omnidirectionally from the ecosystem patches providing cooling effects towards the surrounding areas (e.g., Longato et al., 2023) – were identified, also denominated as service benefitting areas (Dworczyk and Burkhard, 2021). Since the spatial extent of these cooling effects is rather limited in terms of linear distance from the ES providing areas (Geneletti et al., 2022), the service benefitting areas are those located in the immediate surroundings of the ecosystem patches. In this study, standard distances retrieved from the literature were used to map the service benefitting areas, namely 100 linear meters from ecosystem patches with a size of less than 2 ha and 250 linear meters from the bigger ones (Geneletti et al., 2016). This size threshold is typically used to discriminate between smaller ecosystems with a shorter cooling decay effect and the bigger ones being characterized by a larger decay effect (e.g., Majekodunmi et al., 2020; Zardo et al., 2017).

To all the ecosystem patches located within at such a distance that urban areas can benefit from their cooling effects, a distance buffer was applied depending on the size threshold (i.e., 100-m-buffer for ecosystem patches smaller than 2 ha, and 250-m-buffer for ecosystem patches larger than 2 ha) to simulate the cooling decay effect omnidirectionally radiating from the ES providing areas. To capture the different intensities of the cooling effects potentially provided by different types of ecosystems, each buffer is assigned the corresponding ES potential score of the providing ecosystem patch that generated it (i.e., the higher the ES potentialof an ecosystem patch, the higher the intensity potential of its cooling effect in the benefit-

Spatial distribution of the average LST summer values (reference period: 2013-2022) in the urban area of Udine
Credits: elaboration of the authors
Fig. 2

ting areas). When an area is covered by two or more buffers (i.e., an area can benefit from the cooling effects provided by two or more ecosystem patches), the highest ES potential score is assigned to that area to capture the maximum benefit.

Finally, scores from 1 to 5 – corresponding to the decreasing capacity to cope with the adverse effects of UHI – are assigned to allocate the worst condition (i.e., lack of coping capacity: score of 5) to areas not benefitting from any cooling effect, and the best condition (i.e., highest coping capacity: score of 1) to areas benefitting from the most intense cooling effect (Table 2).

Once assessed the two factors, they were combined using the method of weighted sum to obtain the final vulnerability condition. A higher (relative) weight was assigned to the factor related to the urban land surface's contribution in determining the UHI phenomenon mapped through the LST (weight of 0.6 versus weight of 0.4 assigned to the factor related to the cooling benefits). This is justified by the fact that, especially during the night when the UHI phenomenon is more evident, it was statistically proved that the most relevant factor influencing the trend of temperatures in urban areas is the presence and amount of man-made impervious surfaces, namely those most likely to accumulate heat, while vegetation and its mitigation effects have a relatively lower influence (Ziter et al., 2019; Yan et al., 2014). This is somewhat confirmed by the findings of other authors who assessed the relative contribution of potential factors that may influence UHI intensity and/or cooling effects of green areas. For example, Naserikia and colleagues (2022) found that in tropical, cold, and temperate climates (the latter is the background climate of the case study area), the share of built-up impervious surfaces is the strongest contributor to LST variability during warm months followed by the presence of vegetation. In another recent study (Liu et al., 2023), it was showed that the factors related to the proportion of built-up land within and in the surrounding of urban green spaces, if considered altogether, may statistically have a higher influence on the cooling profile of such spaces compared to the factors related to vegetation (e.g., patch density and tree cover share).

The formula used to combine the two factors is the following:

$V_{UHI} = (F_{LST} * 0.6) + (F_{C} * 0.4)$

where V_{UHI} indicates the vulnerability in relation to the propensity of urban areas to suffer from UHI effects, F_{LST} indicates the factor related to the urban land surface's contribution in determining the UHI phenomenon (i.e., 'sensitivity' factor), F_{C} indicates the factor related to the cooling benefits provided by ecosystems (i.e., 'coping capacity' factor).

The result of this operation allows to spatially-explicit map the final vulnerability indicator, with vulnerability scores ranging from 1 (lowest vulnerability condition) to 5 (highest vulnerability condition).

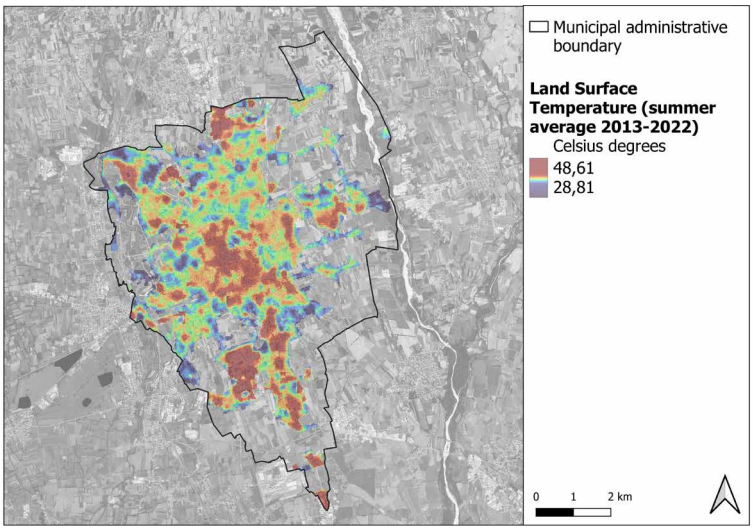

Results

Concerning the urban land surface's contribution in determining the UHI phenomenon, Figure 2 shows the spatial distribution of the average LST summer values (years 2013-2022) elaborated for the case study area.

The spatial variability of temperature values highlights that the higher temperatures are especially recorded in the historic city center and immediate south-eastern surroundings, characterized by a high proportion of sealed soil with high building density and narrow streets, and an almost absence of green elements, as well as in the highly impervious (i.e., characterized by large building footprints and car parking areas) industrial areas that can be especially found towards the southern and northern periphery. Cooler spots correspond to green urban areas, as well as to low-density residential neighborhoods (i.e., extensively characterized by private gardens) diffusely located in the areas external the city center.

When converting these values into scores depicting the sensitivity to UHI (Figure 3), the role of man-made surfaces in contributing to UHI is even more evident, with industrial areas showing the highest propensity to accumulate a huge amount of heat into the surface.

As regards the factor related to the cooling benefits provided by ecosystems, Figure 4 shows the spatial distribution of the qualitative scores depicting the different potential intensities of the cooling effects within the benefitting areas. Figure 5 instead shows the scores assigned to depict the capacity to cope with the adverse effects of UHI according to the cooling benefits potentially provided in the study area.

Large portions of the central urban area (i.e., historic city center and immediate southern surroundings) cannot benefit from any cooling effect since they are located far away (i.e., more than 100/250 linear meters) from natural or semi-natural ecosystems (including urban green spaces), thus having assigned the worst condition (i.e., the highest score). The greatest benefits in terms of cooling, being consequently as-

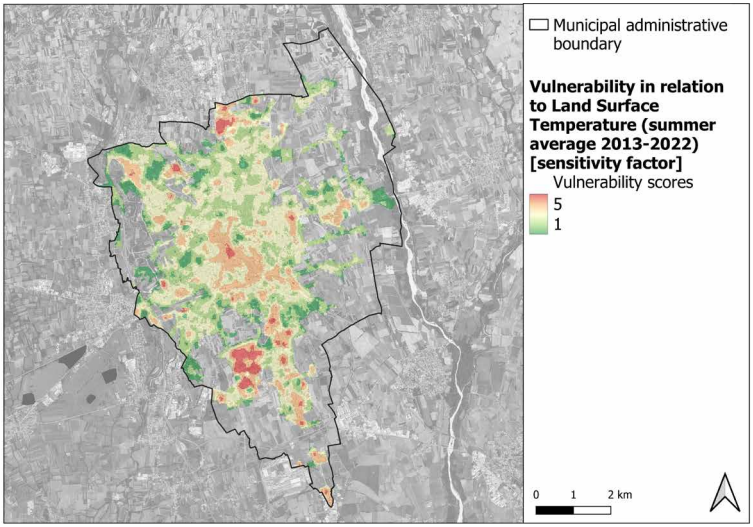
Municipal administrative boundary
Vulnerability in relation to Land Surface Temperature (summer average 2013-2022) [sensitivity factor]
Vulnerability scores
5
1
0 1 2 km

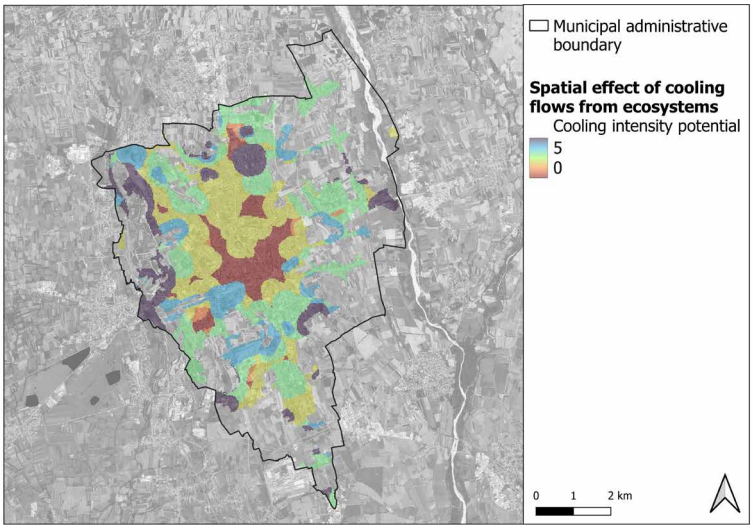
Municipal administrative boundary
Spatial effect of cooling flows from ecosystems
Cooling intensity potential
5
0
0 1 2 km

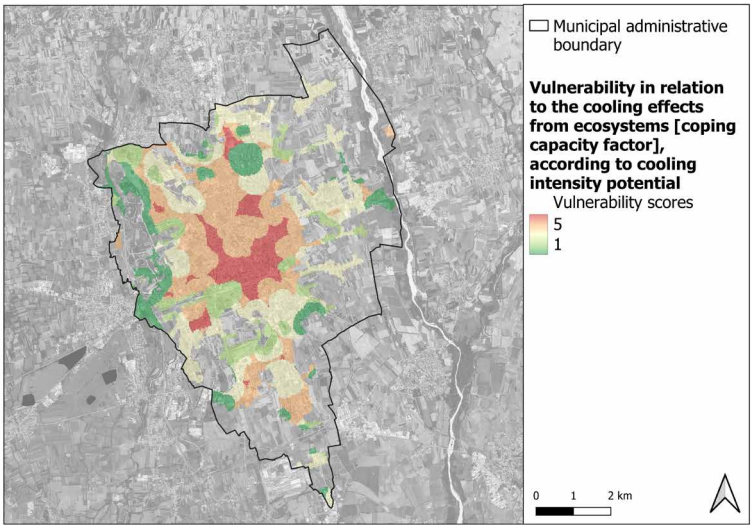
Municipal administrative boundary
Vulnerability in relation to the cooling effects from ecosystems [coping capacity factor], according to cooling intensity potential
Vulnerability scores
5
1
0 1 2 km

Spatial distribution of the scores depicting the vulnerability condition according to the sensitivity factor related to the urban land surface's contribution (i.e., the LST) to UHI (i.e., the higher the score the higher the vulnerability because of the higher sensitivity)
Credits: elaboration of the authors
Fig. 3

Spatial distribution of the qualitative scores depicting the potential intensities of the cooling effects from ecosystems
Credits: elaboration of the authors
Fig. 4

Spatial distribution of the scores depicting the vulnerability condition according to the capacity to cope with the adverse effects of UHI thanks to the cooling effects from ecosystems (i.e., the higher the score the higher the vulnerability because of the lower capacity to cope)
Credits: elaboration of the authors
Fig. 5

sociated with the best condition (i.e., the lowest score), are especially found towards the western urban periphery, located in the proximity of the (relatively large) woodland ecosystem that follows the course of the river flowing west of the city. The few other spots characterized by cooling benefits with high cooling intensity potential are the ones located near the fragmented and dispersed woodland and/or shrubland patches that can be (randomly) found in peri-urban fringes.

The final vulnerability map depicting the propensity to suffer from UHI effects (according to the two factors considered) in the urban area of Udine is presented in Figure 6. More vulnerable areas are found where the worst conditions for both the factors considered overlap. This is especially true for the dense urban core and for some industrial sites located in the southern and northern peri-urban areas that are far away from ecosystem typologies with a high potential to provide cooling benefits.

When comparing the scores obtained in the final vulnerability map with the ones obtained using the LST data only, thus only based on sensitivity to UHI without accounting for the capacity to cope with UHI effects provided by ecosystems (i.e., as done in many LST-based studies, see Introduction), some differences are revealed (Figure 7). It can be noted that the urban areas that are far away from ecosystem patches

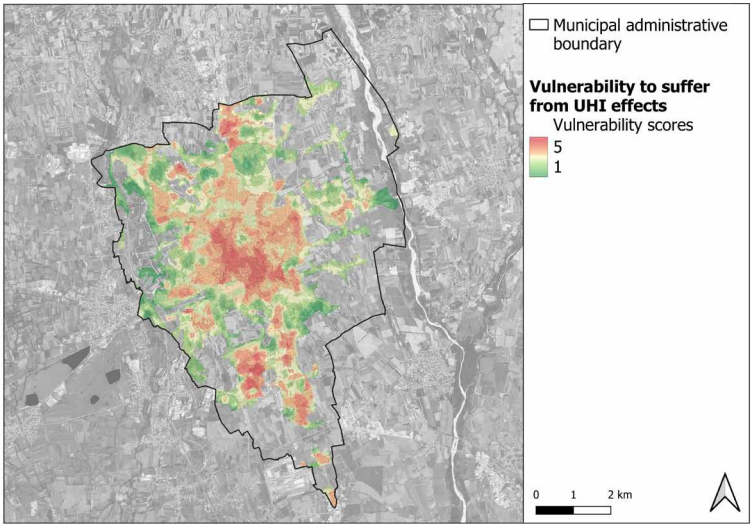

Final vulnerability map with the spatial distribution of the vulnerability scores depicting the propensity to suffer from UHI effects in the urban area of Udine (i.e., the higher the score the higher the vulnerability condition)

Credits: elaboration of the authors

Fig. 6

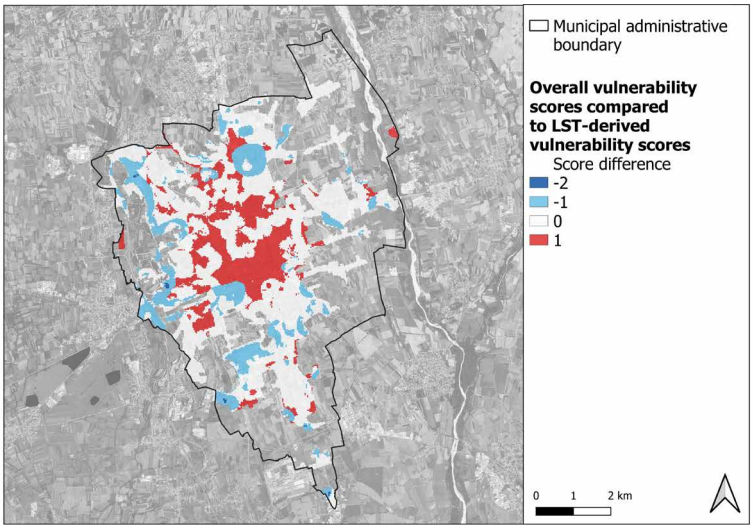

Differences in vulnerability scores between the scores obtained in the final vulnerability map and the ones obtained according to the sensitivity factor only (i.e., the urban land surface's contribution to UHI assessed through the LST shown in Figure 3)

Credits: elaboration of the authors

Fig. 7

Number and percentage of pixels classified into the five scores depicting the vulnerability/sensitivity condition: final vulnerability map (Figure 6), LST-derived sensitivity map (Figure 3), and their difference
Tab. 2

Score depicting the vulnerability/ sensitivity condition	Pixels in LST-derived sensitivity map [1]		Pixels in the final vulnerability map [2]		Pixel difference in % ([1] – [2])
	Number	%	Number	%	
Lowest (1)	3706	11,39	4648	14,28	-2,89
(2)	10272	31,56	8330	25,59	+5,97
(3)	12280	37,73	12845	39,47	-1,74
(4)	5334	16,39	5239	16,10	+0,29
Highest (5)	955	2,93	1485	4,56	-1,63

are characterized by an overall worse condition in the final vulnerability map even if not having the highest LST values (i.e., a higher score of + 1). In parallel, some peripheral areas are instead characterized by an improved condition (i.e., a lower score of -1 or, in some isolated cases, -2), since, despite having among the highest LST values, can benefit from (substantial) cooling effects provided by nearby ecosystem patches. Table 2 reports the number and percentage of pixels broken down per vulnerability/sensitivity condition (according to the associated scores) obtained in the two cases and their comparison. Differences in vulnerability scores between the scores obtained in the final vulnerability map and the ones obtained according to the sensitivity factor only (i.e., the urban land surface's contribution to UHI assessed through the LST shown in Figure 3.

Discussion and conclusions

Urban areas are likely to become 'islands' of higher temperatures compared to outlying rural areas. This difference tends to be more pronounced at night when the UHI phenomenon is more evident. Measurements of LST are important to understand and monitor UHI and their contributing factors due to the large spatial and temporal availability of data. LST data has been extensively used in the literature to assess and map surface UHI in many parts of the world (e.g., Xu et al., 2023; do Nascimiento et al., 2022). However, surface UHI usually does not fully match air UHI since it is not able to properly capture thermal exchange processes occurring above the city's surface, which instead is the main parameter to understand UHI-related thermal discomfort in cities to guide prioritization of mitigation strategies (see the Introduction section for more information).

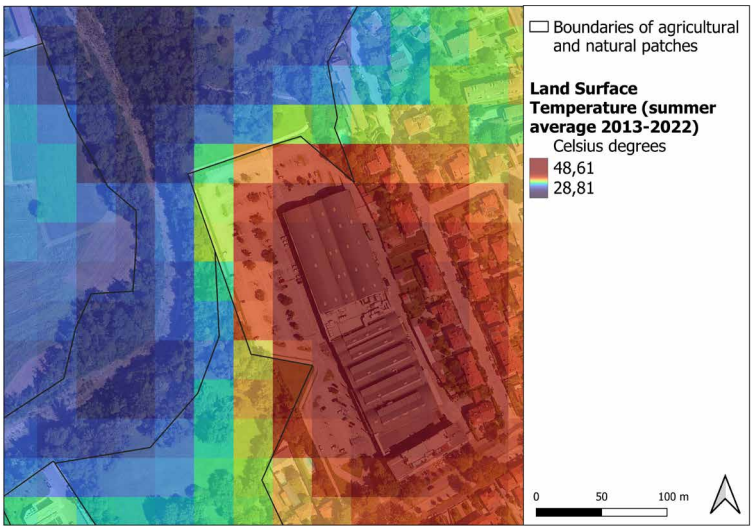

Zoom-in map showing the LST distribution across a rural-urban interface area

Credits: elaboration of the authors

Fig. 6

In this study, a simple and quick method that combines measurements of LST depicting land surface's contribution to UHI (i.e., sensitivity to UHI) with the spatial effects of the local climate mitigation ES provided by ecosystems is proposed to enhance the quality of LST-based UHI assessments. This way, cooling spatial effects of natural and semi-natural ecosystems that instead are not (fully) accounted for by LST are captured, accounting for the capacity to cope with the adverse effects of UHI provided by ecosystems. The method is applied in the city of Udine (Italy) to map the vulnerability profile of the city in relation to its propensity to suffer from (more or less intense) UHI effects.

As a matter of fact, Figure 8 shows a zoom-in map with the LST distribution in a rural-urban interface area where two contrasting conditions are contiguous: the likely-coolest ecosystem type (i.e., a woodland area) and the likely-warmest urban land cover type (i.e., a highly impervious industrial site). It can be noted that immediately beyond the border of the wooded patch, the pavement and building areas of the industrial site show significantly higher surface temperatures, shifting from about 35° (in the wooded pixels located near the border with the industrial site) to 42° in few tens of meters (1 to 2 pixels, which resolution is 30 meters), which is a value in line with those found in other industrial sites not bordering with any vegetated patch. For this reason, accounting for the cooling spatial effects of ecosystem patches can improve the assessment by discriminating between urban hot areas that however are relatively close to ES providing areas and that can thus benefit from their cooling effects and the ones that are similarly hot but cannot benefit from this ES. As shown in the Results section, adding this second factor partially modifies the vulnerability profile of the city compared to using solely the LST data. In particular, in our proposed method

many peri-urban areas were assigned a lower vulnerability condition compared to the assessment based on the LST data only, especially in the western side of the city located near a relatively large woodland area, while the contrary occurred in the dense urban city center with many areas that were assigned a higher vulnerability condition. This is (partly) in line with the results of studies that used more sophisticated methods. For example, Steigerwald and colleagues (2022) used a climate model to assess the benefits of cooling processes promoted by natural and seminatural ecosystems (i.e., 'cold air formation areas') in reducing nocturnal urban temperatures in a medium-sized city in Germany. They found that the city's 'thermal hotspots' (i.e., areas with the highest air temperatures) cover the majority of the central areas characterized by dense or very dense urban fabric (65% to 93%) since they cannot benefit from the cooling effects flowing from the surrounding countryside, where most of the 'cold air formation areas' are located. Instead, more than half of the industrial areas were not included within the 'thermal hotspot' areas, despite being among the most problematic land covers in terms of surface heat accumulation, given their proximity to extra-urban 'cold air formation areas' (such as in Udine). Similar results were found by Schwarz and colleagues (2012), who measured air temperatures through mobile measurements during night hours and found that built-up areas showing similar characteristics were characterized by higher or lower temperatures (also) according to their greater or shorter distance to green spaces, respectively.

This is an important element to consider when developing mapping tools aimed at spatially assessing vulnerability to UHI in cities, since when these maps are used as a decision support system to guide spatial allocation and prioritization of solutions to mitigate UHI effects in cities, the resulting spatial variability of the different vulnerability conditions will affect the decision towards one rather than another area to prioritize for their implementation.

In this sense, possible adaptation actions that can be implemented include, for example, the creation of new green areas (e.g., pocket parks, urban afforestation), the heat-resilient renovation of public squares and parking lots (e.g., de-sealing actions, cool pavements, public greenery), the adaptation of existing streets (e.g., street trees, cooler materials instead of asphalt, more permeable surfaces), and the greening of infrastructures and buildings (e.g., green roofs and walls, cool roofs, linear green corridors along transport infrastructures) (Petsinaris et al., 2020). While most of the measures require available ground space to be implemented (e.g., Longato et al., 2023), within the most compact urban areas (i.e., very little or no infill space available, no garden areas, highest building density, and narrow streets) – which are among the ones typically showing among the highest vulnerability to UHI, such as

in Udine – interventions that do not require new space on the ground (e.g., greening buildings or de-sealing actions in existing public spaces) are extremely important (e.g., Langemeyer et al., 2020; Venter et al., 2021b). A rapid visual analysis of the urban built form of Udine reveals that, in the most vulnerable areas, opportunities to mitigate UHI are mainly related to green (or cool) roof installation in private residential buildings and de-paving and/or greening actions (i.e., more tree-covered spaces) in public spaces (e.g., squares) in the city center. The same actions could be promoted in private industrial buildings and large pavement areas in the peri-urban industrial sites, together with increasing the potential of surrounding ecosystems to cool down temperatures through, e.g., green-belt-likely re-naturalization projects in the urban fringes.

The limitations of the study mainly involve the rather simplified method used for assessing the cooling effects that is just based on standard values from the literature for both the distance decay function and the ES potential scores from which is derived the cooling intensity potential profile. This latter aspect, in addition, relies on land use and cover maps which resolution and accuracy are not always good enough to depict all the urban green spaces (e.g., smaller green patches, private gardens), which instead are usually among the most widespread green space typologies that can be found in a city and which play a great role in ES delivery, including in mitigating local temperatures (Balzan et al., 2021). Possible improvements of the method may include the assessment of distance decay functions and cooling intensity profiles that rely not only on ecosystem types but on more specific ecosystem characteristics that may contribute to influencing both the spatial extent and the intensity of the cooling effects they provide (e.g., vegetation structure, ecosystem condition, patch shape, etc.) (e.g., Gallay et al., 2023; Zhou et al., 2023; Fu et al., 2022; Aram et al., 2019). However, the method proposed in this study can have the advantage of being easier to use and more understandable than (more) complex methods (i.e., less demanding in data collection and elaboration) by decision-makers working in everyday planning practices and routines, as well as being in principle replicable in any other city. To this aim, it has to be noted that, while LST data are provided worldwide, and thus can be easily obtained for any city, the assessment of the cooling benefits provided by the ecosystems depends on the availability of suitable land use and cover maps, which not always can be easily obtained (at least with an accuracy/resolution that is sufficiently good enough). However, methods for deriving/improving land use and cover maps exist through satellite data and can be applied in data-scarce environments (e.g., Balzan et al., 2021). Furthermore, the land-cover-based ES scores used in this study are specifically tailored to the Corine Land Cover classification system. To directly ap-

ply them, a land use and cover map that uses this classification system or that can be rather easily re-classified according to it (such as in the case study presented) is needed. Contrary, other more suitable ES-based scoring matrices may be searched and applied (e.g., see Adem Esmail et al., 2023)) or a new one can be developed involving local experts to tailor the ES scores to the specific case study (Campagne et al., 2020).

Another field deserving future work to further advance the proposed method is related to the combination of the UHI vulnerability assessment with sociodemographic data about the distribution of population within the city and its socio-demographic and economic profile. Adding this type of data enables the integration of heat vulnerability and exposure (i.e., the exposed elements that can be harmed, in this case by high temperatures exacerbated by UHI effects) metrics that can be used to better target the urban areas where the implementation of mitigation measures could provide benefits to both a larger number of beneficiaries (i.e., areas that combine a high vulnerability with a high-density resident population) and to the population groups that are more vulnerable to heat stress (e.g., areas with higher rates of children and elderly, economically disadvantage people, etc.) (e.g., Tieskens et al., 2022).

This way, also the demand for ES is used to inform decision-making in prioritizing urban areas where greenspace interventions can have the most (positive) impact, which is one of the main gaps in the field of ES science application in spatial planning (Longato et al., 2021). However, it has to be noted that different approaches for assessing the demand can be used depending on the scope of the assessment and the groups of beneficiaries that one is willing to target. For example, using only the resident population as the target beneficiary group can lead to neglecting industrial areas. In some cases, multiple exposure and vulnerability metrics related to different aspects of the city life and to different city users (e.g., resident population, public service areas attracting people and/or more disadvantaged groups such as schools and hospitals, areas in which people work such as industrial sites, etc.) can be used and combined, perhaps by weighting them in terms of relative importance/relevance according to empirical evidence or political willingness, to account for multiple beneficiaries' demand profiles.

Acknowledgments

This study was supported by the Friuli Venezia Giulia Region (*Regione Autonoma Friuli Venezia Giulia*) under the framework of the Operative Agreement "*Accordo operativo con il Servizio Pianificazione Paesaggistica, Territoriale e Strategica per attività di supporto scientifico e metodologico alla predisposizione di una Variante al Piano del Governo del Territorio (PGT) relativamente all'introduzione della tematica di adattamento al Cambiamento Climatico e Resilienza Territoriale negli strumenti urbanistici di area vasta*".

References

Adem Esmail B., Cortinovis C., Wang J., Geneletti D., Albert C. 2023, *Mapping and assessing ecosystem services for sustainable policy and decision-making in Eritrea, Ambio*, vol. 52, 1022–1039. https://doi.org/10.1007/s13280-023-01841-4

Aflaki A., Mirnezhad M., Ghaffaraianhoseini A., Ghaffarianhoseini A., Omrany H., Wang Z.-H., Akbari H. 2017, *Urban heat island mitigation strategies: A state-of-the-art review on Kuala Lumpur, Singapore and Hong Kong, Cities*, vol. 62, 131–145. https://doi.org/10.1016/j.cities.2016.09.003

Aram F., Higueras García E., Solgi E., Mansournia S. 2019, *Urban green space cooling effect in cities, Heliyon*, vol. 5, n. 4, e01339. https://doi.org/10.1016/j.heliyon.2019.e01339

Azevedo J.A., Chapman L., Muller C.L. 2016, *Quantifying the daytime and night-time urban heat Island in Birmingham, UK: A comparison of satellite derived land surface temperature and high resolution air temperature observations, Remote Sensing*, vol. 8, n. 2. https://doi.org/10.3390/rs8020153

Balzan M., Zulian G., Maes J., Borg M. 2021, *Assessing urban ecosystem services to prioritise nature-based solutions in a high-density urban area, Nature-Based Solutions*, vol. 1, 100007. https://doi.org/10.1016/j.nbsj.2021.100007

Bird D.N., Banzhaf E., Knopp J., Wu W., Jones L. 2022, *Combining Spatial and Temporal Data to Create a Fine-Resolution Daily Urban Air Temperature Product from Remote Sensing Land Surface Temperature (LST) Data, Atmosphere*, vol. 13, 1152. https://doi.org/10.3390/atmos13071152

Burkhard B., Kandziora M., Hou Y., Müller F. 2014, *Ecosystem Service Potentials, Flows and Demands – Concepts for Spatial Localisation, Indication and Quantification, Landscape Online*, vol. 34, 1-32. https://doi.org/10.3097/LO.201434

Campagne C. S., Roche P., Müller F., Burkhard B. 2020, *Ten years of ecosystem services matrix: Review of a (r)evolution, One Ecosystem*, vol. 5. https://doi.org/10.3897/oneeco.5.e51103

do Nascimento A.C.L., Galvani E., Gobo J.P.A., Wollmann C.A. 2022, *Comparison between Air Temperature and Land Surface Temperature for the City of São Paulo, Brazil, Atmosphere,* vol. 13, 491. https://doi.org/10.3390/atmos13030491

Dworczyk C., Burkhard B. 2021, *Conceptualising the demand for ecosystem services – an adapted spatial-structural approach, One Ecosystem*, vol. 6, e65966. https://doi.org/10.3897/oneeco.6.e65966

Gallay I., Olah B., Murtinová V., Gallayová Z., 2023, *Quantification of the Cooling Effect and Cooling Distance of Urban Green Spaces Based on Their Vegetation Structure and Size as a Basis for Management Tools for Mitigating Urban Climate, Sustainability*, vol. 15, 3705. https://doi.org/10.3390/su15043705

Geneletti D., Zardo L., Cortinovis C. 2016, *Promoting nature- based solutions for climate adaptation in cities through impact assessment, in D. Geneletti (ed.), Handbook on biodiversity and ecosystem services in impact assessment*, Edward Elgar Publishing, Cheltenham, UK – Northampton, MA, USA, 428-452. https://doi.org/10.4337/9781783478996.00025

Geneletti D., Cortinovis C., Orta-Ortiz M.S., Kato-Huerta J., Longato D., Falco E. 2022, *Mainstreaming Nature-Based Solutions in Cities Through Performance-Based Planning: A Case Study in Trento, Italy*, in I.H. Mahmoud, E. Morello, F.L. de Oliveira, D. Geneletti (eds.), Nature-based Solutions for Sustainable Urban Planning. Greening Cities, Shaping Cities, Springer, 19–46. https://doi.org/10.1007/978-3-030-89525-9_2

Goldenberg R., Kalantari Z., Destouni, G. 2021, *Comparative quantification of local climate regulation by green and blue urban areas in cities across Europe, Sci Rep*, vol. 11, 23872. https://doi.org/10.1038/s41598-021-03140-y

Fu j., Dupre K., Tavares S., King D., Banhalmi-Zakar Z. 2022, *Optimized greenery configuration to mitigate urban heat: A decade systematic review, Frontiers of Architectural Research*, vol. 11, 466-491. https://doi.org/10.1016/j.foar.2021.12.005

IPCC 2007, *Climate Change 2007: Impacts, Adaptation and Vulnerability: Contribution of Working Group II to the Fourth Assessment Report of the Intergovernmental Panel on Climate Change*. Cambridge University Press, Cambridge, UK.

IPCC 2014, *Climate Change 2014: Impacts, Adaptation, and Vulnerability. Part A: Global and Sectoral Aspects. Contribution of Working Group II to the Fifth Assessment Report of the Intergovernmental Panel on Climate Change*, Cambridge University Press, Cambridge, United Kingdom and New York, NY, USA.

ISTAT 2023, *Bilancio demografico mensile e popolazione residente per sesso*, anno 2023, < https://demo.istat.it/app/?a=2023&i=D7B> (12/2023).

Kim J., Lee D.-K., Brown R.B., Kim S., Kim J.-H., Sung S. 2022, *The effect of extremely low sky view factor on land surface temperatures in urban residential areas, Sustainable Cities and Society*, vol. 80, 103799. https://doi.org/10.1016/j.scs.2022.103799

Langemeyer J., Wedgwood D., McPhearson T., Baró F., Madsen A.L., Barton D.N. 2020, *Creating urban green infrastructure where it is needed – A spatial ecosystem service-based decision analysis of green roofs in Barcelona, Science of the Total Environment*, vol. 707, 135487. https://doi.org/10.1016/j.scitotenv.2019.135487

Liu Z., Fu L., Wu C., Zhang Z., Zhang Z., Lin X., Li X., Hu Y., Ge H. 2023, *Spatialized importance of key factors affecting park cooling intensity based on the park scale, Sustainable Cities and Society*, Vol. 99, 104952. https://doi.org/10.1016/j.scs.2023.104952.

Longato D., Cortinovis C., Albert C., Geneletti D. 2021, *Practical applications of ecosystem services in spatial planning: Lessons learned from a systematic literature review, Environmental Science and Policy*, vol. 119, 72–84. https://doi.org/10.1016/j.envsci.2021.02.001

Longato D., Cortinovis C., Balzan M., Geneletti D. 2023, *A method to prioritize and allocate nature-based solutions in urban areas based on ecosystem service demand, Landscape and Urban Planning*, vol. 235, 104743. https://doi.org/10.1016/j.landurbplan.2023.104743

Majekodunmi M., Emmanuel R., Jafry T. 2020, *A spatial exploration of deprivation and green infrastructure ecosystem services within Glasgow city, Urban Forestry and Urban Greening*, vol. 52, 126698. https://doi.org/10.1016/j.ufug.2020.126698

Maragno D., Gaglio M., Robbi K., Appiotti F., Fano E.A., Gissi E. 2018, Fine-scale analysis of urban flooding reduction from green infrastructure: An ecosystem services approach for the management of water flows, Ecological Indicators, vol. 386, 1-19. https://doi.org/10.1016/j.ecolmodel.2018.08.002

Naserikia M., Hart M.A., Nazarian N., Bechtel B. 2022, *Background climate modulates the impact of land cover on urban surface temperature, Sci Rep*, vol. 12, 15433. https://doi.org/10.1038/s41598-022-19431-x

Oke T.R., Mills G., Christen A., Voogt J.A. 2017, *Urban Climates*, Cambridge University Press.

Park C.Y., Park Y.S., Kim H.G., Yun S.H., Kim C.-K. 2021, *Quantifying and mapping cooling services of multiple ecosystems, Sustainable Cities and Society,* vol. 73, 103123. https://doi.org/10.1016/j.scs.2021.103123

Park J.-H., Cho G.-H. 2016, *Examining the Association between Physical Characteristics of Green Space and Land Surface Temperature: A Case Study of Ulsan, Korea, Sustainability*, vol. 8(8):777. https://doi.org/10.3390/su8080777

Parker D.E. 2010, *Urban heat island effects on estimates of observed climate change, Wiley Interdisciplinary Reviews: Climate Change*, vol. 1, n. 1, 123–133. https://doi.org/10.1002/wcc.21

Parry M.L., Canziani O.F., Palutikof J.P., van der Linden P.J., Hanson C.E. (eds.), 2007, *Contribution of Working Group II to the Fourth Assessment Report of the Intergovernmental Panel on Climate Change*. Cambridge and New York: Cambridge University Press.

Pena Acosta M., Vahdatikhaki F., Santos J., Dorée A.G. 2023, *A comparative analysis of surface and canopy layer urban heat island at the micro level using a data-driven approach, Sustainable Cities and Society*, vol. 99, 104944. https://doi.org/10.1016/j.scs.2023.104944

Petsinaris F., Baroni L., Birgit G. 2020, *Compendium of Nature-based and 'grey' solutions to address climate- and water-related problems in European cities*. Grow Green Project.

Reiners P., Sobrino J., Kuenzer C. 2023, Satellite-Derived *Land Surface Temperature Dynamics in the Context of Global Change—A Review, Remote Sensing*, vol. 15, 1857. https://doi.org/10.3390/rs15071857

Schwarz N., Schlink U., Franck U., Großmann K. 2012, *Relationship of land surface and air temperatures and its implications for quantifying urban heat island indicators—an application for the city of Leipzig (Germany), Ecological Indicators*, vol. 18, 693–704. https://doi.org/10.1016/j.ecolind.2012.01.001

Shiflett S.A., Liang L.Y.L., Crum S.M., Feyisa G.L., Wang J., *Jenerette G.D. 2017, Variation in the urban vegetation, surface temperature, air temperature nexus, Sci. Total Environ.*, vol. 579, 495–505. https://doi.org/10.1016/j.scitotenv.2016.11.069

Spronken-Smith R.A., Oke T.R. 1999, *Scale modelling of nocturnal cooling in urban parks. Bound. Layer Meteorol.*, vol. 93, 287–312. https://doi.org/10.1023/A:1002001408973

Steigerwald F., Kossmann M., Schau-Noppel H., Buchholz S., Panferov O. 2022, *Delimitation of Urban Hot Spots and Rural Cold Air Formation Areas for Nocturnal Ventilation Studies Using Urban Climate Simulations, Land*, vol. 11, 1330. https://doi.org/10.3390/land11081330

Sun T., Sun R., Chen L. 2020, *The Trend Inconsistency between Land Surface Temperature and Near Surface Air Temperature in Assessing Urban Heat Island Effects, Remote Sensing*, vol. 12(8), 1271. https://doi.org/10.3390/rs12081271

Tang L., Zhang Q., Fan Y., Liu H., Fan Z. 2023, *Exploring the impacts of greenspace spatial patterns on land surface temperature across different urban functional zones: A case study in Wuhan metropolitan area, China, Ecological Indicators*, vol. 146, 109787. https://doi.org/10.1016/j.ecolind.2022.109787

Tieskens K.F., Smith I.A., Jimenez R.B., Hutyra L.R., Fabian M.P. 2022, *Mapping the gaps between cooling benefits of urban greenspace and population heat vulnerability, Science of the Total Environment*, vol. 845, 157283. https://doi.org/10.1016/j.scitotenv.2022.157283

UN 2016, *Report of the open-ended intergovernmental expert working group on indicators and terminology relating to disaster risk reduction*, United Nations General Assembly, Seventy-first session, Agenda item 19 (c), Sustainable development: disaster risk reduction.

Vaz Monteiro M., Doick K.J., Handley P., Peace A. 2016, *The impact of greenspace size on the extent of local nocturnal air temperature cooling in London, Urban Forestry & Urban Greening*, vol. 16, 160–169. https://doi.org/10.1016/j.ufug.2016.02.008

Venter Z.S., Chakraborty T., Lee X. 2021, *Crowdsourced air temperatures contrast satellite measures of the urban heat island and its mechanisms, Sci Adv.*, vol. 26;7. doi: 10.1126/sciadv.abb9569.

Venter Z.S., Barton D.N., Martinez-Izquierdo L., Langemeyer J., Baró F., McPhearson T. 2021b, *Interactive spatial planning of urban green infrastructure – Retrofitting green roofs where ecosystem services are most needed in Oslo, Ecosystem Services*, vol. 50. https://doi.org/10.1016/j.ecoser.2021.101314

Walawender J.P., Szymanowski M., Hajto M.J., Bokwa A. 2014, *Land Surface Temperature Patterns in the Urban Agglomeration of Krakow (Poland) Derived from Landsat-7/ETM+ Data, Pure Appl. Geophys.*, vol. 171, 913–940. https://doi.org/10.1007/s00024-013-0685-7

Wei X., Wang X.-J. 2022, *Analyzing the Spatial Distribution of LST and Its Relationship With Underlying Surfaces in Different Months by Classification and Intersection, Front. Environ. Sci.*, vol. 10, 872282. https://doi.org/10.3389/fenvs.2022.872282

Xiang Y., Zheng B., Bedra K.M., Ouyang Q., Liu J., Zheng J. 2023, *Spatial and seasonal differences between near surface air temperature and land surface temperature for Urban Heat Island effect assessment, Urban Climate*, vol. 52, 101745. https://doi.org/10.1016/j.uclim.2023.101745

Xu Z., Zhao S. 2023, *Scale dependence of urban green space cooling efficiency: A case study in Beijing metropolitan area, Science of The Total Environment*, vol. 898, 165563. https://doi.org/10.1016/j.scitotenv.2023.165563

Yan H., Fan S., Guo C., Hu J., Dong L. 2014, *Quantifying the Impact of Land Cover Composition on Intra-Urban Air Temperature Variations at a Mid-Latitude City, PLoS ONE*, vol. 9(7). https://doi.org/10.1371/journal.pone.0102124

Yu Z., Yang G., Zuo S., Jørgensen G., Koga M., Vejre H. 2020, *Critical review on the cooling effect of urban blue-green space: A threshold-size perspective, Urban Forestry & Urban Greening*, vol. 49, 126630. https://doi.org/10.1016/j.scs.2023.104952

Zardo L., Geneletti D., Pérez-Soba M., Van Eupen M. 2017, *Estimating the cooling capacity of green infrastructures to support urban planning, Ecosystem Services*, vol. 26, 225–235. https://doi.org/10.1016/j.ecoser.2017.06.016

Zhou Y., Feng Z., Xu K., Wu K., Gao H., Liu P. 2023, *Ecosystem Service Flow Perspective of Urban Green Land: Spatial Simulation and Driving Factors of Cooling Service Flow, Land*, vol. 12, 1527. https://doi.org/10.3390/land12081527

Ziter C.D., Pedersen E.J., Kucharik C.J., Turner M.G. 2019, *Scale-dependent interactions between tree canopy cover and impervious surfaces reduce daytime urban heat during summer, PNAS*, vol. 116, n. 15, 7575-7580. https://doi.org/10.1073/pnas.1817561116

Web references

ARPA FVG 2023, *Il Clima del Friuli Venezia Giulia*, <https://www.osmer.fvg.it/clima/clima_fvg/02_documenti_descrittivi,_report_e_approfondimenti/01_Il_clima_del_Friuli_Venezia_Giulia/clima_fvg-divulgativo.pdf> (10/2023)

European Topic Centre on Biological Diversity, *A crosswalk between EUNIS habitats Classification and Corine Land Cover*, <https://www.eea.europa.eu/data-and-maps/data/eunis-habitat-classification-1/documentation/eunis-clc.pdf> (10/2023)